Max-Planck-Institut für Plasmaphysik

Local Radiated Power Sensitivity and Intrinsic Impurity Correlation Analysis at the Stellarator Wendelstein 7-X

P. Hacker[1,2]*, D. Zhang[1], F. Reimold[1], R. Burhenn[1] and T. Klinger[1], for the Wendelstein 7-X Team-Collaboration[1]

[1]Max Planck Institute for Plasma Physics, Wendelsteinstr. 1, D-17491 Greifswald, Germany,
[2]Ernst-Moritz-Arndt University Greifswald, Rubenowstr. 1, D-17489 Greifswald, Germany

Bolometer Diagnostic

Goals

- investigate total radiation powerloss through impurities and its distribution
- global & local power balance, as well as impurity and transport studies through tomographic inversion
- real time plasma feedback control based off of the radiation power loss and its distribution to achieve improved detachment, adjust thermal loads of in-vessel components & explore high radiation scenarios

Motivation

- averaged thermal load of in-vessel components expected to be up to 100 kW/m^2 mainly by radiation and non-absorbed heating power
- calculating temporal and spatial evolution of the radiation loss previously only after the plasma has been terminated
- investigate radiation scaling, i.e. importance of intrinsic & extrinsic impurities and their location

Design

- multi-device system: horizontal bolometer camera (HBC, 32 channels) and vertical bolometer camera (VBC, 20 channels for each of two subdetectors) $\Rightarrow$ more detectors with different filters/coatings available, e.g. for investigation of soft x-ray radiation
- steady state operation at discharges with up to 30 min of 10 MW heating power ensured by cooling system with graphite elements and water cooling structures
- detectors are carbon coated Au-foil on 5 µm Si_3N_4 substrate, backed by a 30 µm platin meander with a 0.25 ms response time; temporal resolution of 0.8 ms to 6.4 ms

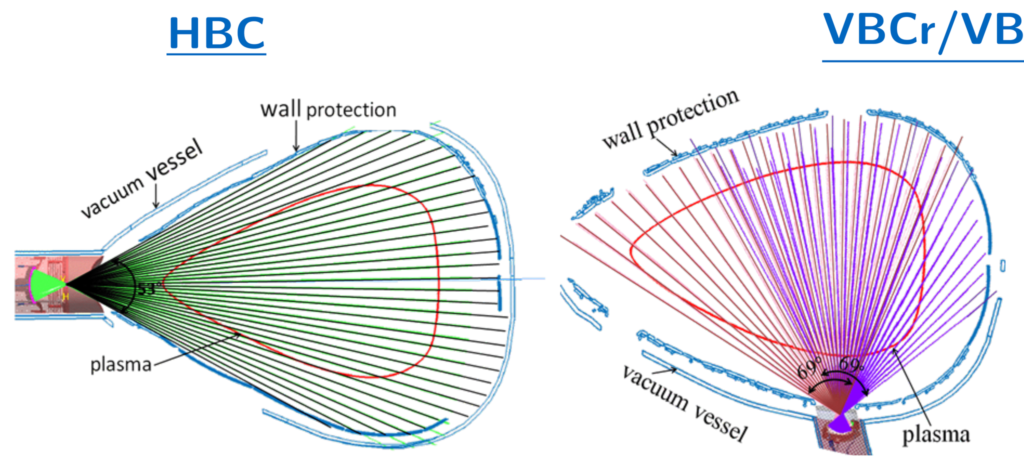

LOS for HBC (32 ch.) and VBC (two 20-ch. subdetector arrays) with individual apertures, retracted into the vacuum vessel behind wall elements; located in the triangle-shaped plane at W7-X.[1]

Equations

The radiation power observed by the bolometers equals to:

$$P_{\text{rad,bolo}} \propto \sum_Z n_e \cdot n_Z \cdot L_Z\,(T_e, T_i, T_Z, \ \ldots)$$

where L_Z is the line radiation function by species Z. For each channel the observed power P_{ch} can be calculated by using[2]:

$$P_{\text{ch}} = F_{\text{ch}} \cdot \left(\tau_{\text{ch}} \frac{\mathrm{d}(\Delta U)}{\mathrm{d}t} + f_{\tau,\text{ch}} \cdot (\Delta U) \right)$$

with $\Delta U \propto \Delta T \propto \Delta P$ the change in measurement voltage, absorber temperature and incident radiation power. Properties denoting $(\cdot)_{\text{ch}}$ refer to the individual channel/foil characteristics, e.g. cooling time (τ) and $f_{\tau,\text{ch}}$, F_{ch} numbers calculated from cable attributes, detector resistance and heat capacity.

Global Power Estimate:

For each camera (VBC, HBC) individually, the total radiation loss can be calculated like:

$$P_{\text{rad, cam}} = \frac{V_{\text{P,tor}}}{V_{\text{cam}}} \cdot \sum_{\text{ch}}^{\text{cam}} \frac{V_{\text{ch}}}{K_{\text{ch}}} \cdot \frac{P_{\text{ch}}}{53\%}$$

with:

$$V_{\text{cam}} = \sum_{\text{ch}} V_{\text{ch}} \ .$$

The volume and geometry of the detectors lines of sight and corresponding aperture are noted as V_{ch}, K_{ch} hence V_{cam} is the total volume investigated by a camera. Using EMC3-Eirene simulation the estimated plasma volume from which radiation is emitted is approximated to be $V_{\text{P, tor}}$.

Real Time Prediction:

Due to technical limitations, feedback was only possible to be calculated based off of a selection S of lines of sights instead of a full array. $\widetilde{P}_{\text{ch}}$ notes a 10-sample average to suppress noise without sacrificing temporal responsiveness:

$$P_{\text{pred}} = P_{\text{rad,S}} = \frac{V_{\text{P}}}{V_{\text{S}}} \cdot \sum_{\text{ch}}^{\text{S}} \frac{V_{\text{ch}}}{K_{\text{ch}}} \cdot \frac{\widetilde{P}_{\text{ch}}}{53\%} \qquad (1) \ .$$

References

[1] "Design Criteria of the Bolometer diagnostic for steady-state operation of the W7-X stellarator"; Zhang, D. et al.; Review of Scientific Instruments, Jan 1st, 2010; DOI:10.1063/1.3483194

[2] "Derivation of bolometer equations relevant to operation in fusion experiments"; Gianone, L. et al.; Review of Scientific Instruments; 20th of November, 2002; DOI: 10.1063/1.1498906

Real Time Feedback

- during last experiment campaign *OP1.2b*: real time plasma feedback control using in-situ calibrations and measurements of radiation loss distribution
- actuator is fast, thermal He-beam valve - gas flow adjusted for target where $P_{\text{rad}} \sim f(n_e, T_e, \ldots)$.
- during experimental campaign used selection $\widetilde{S}_5$ based on an *educated guess* with 5 channels covering the plasma core, edge and *scrape-off layer* SOL

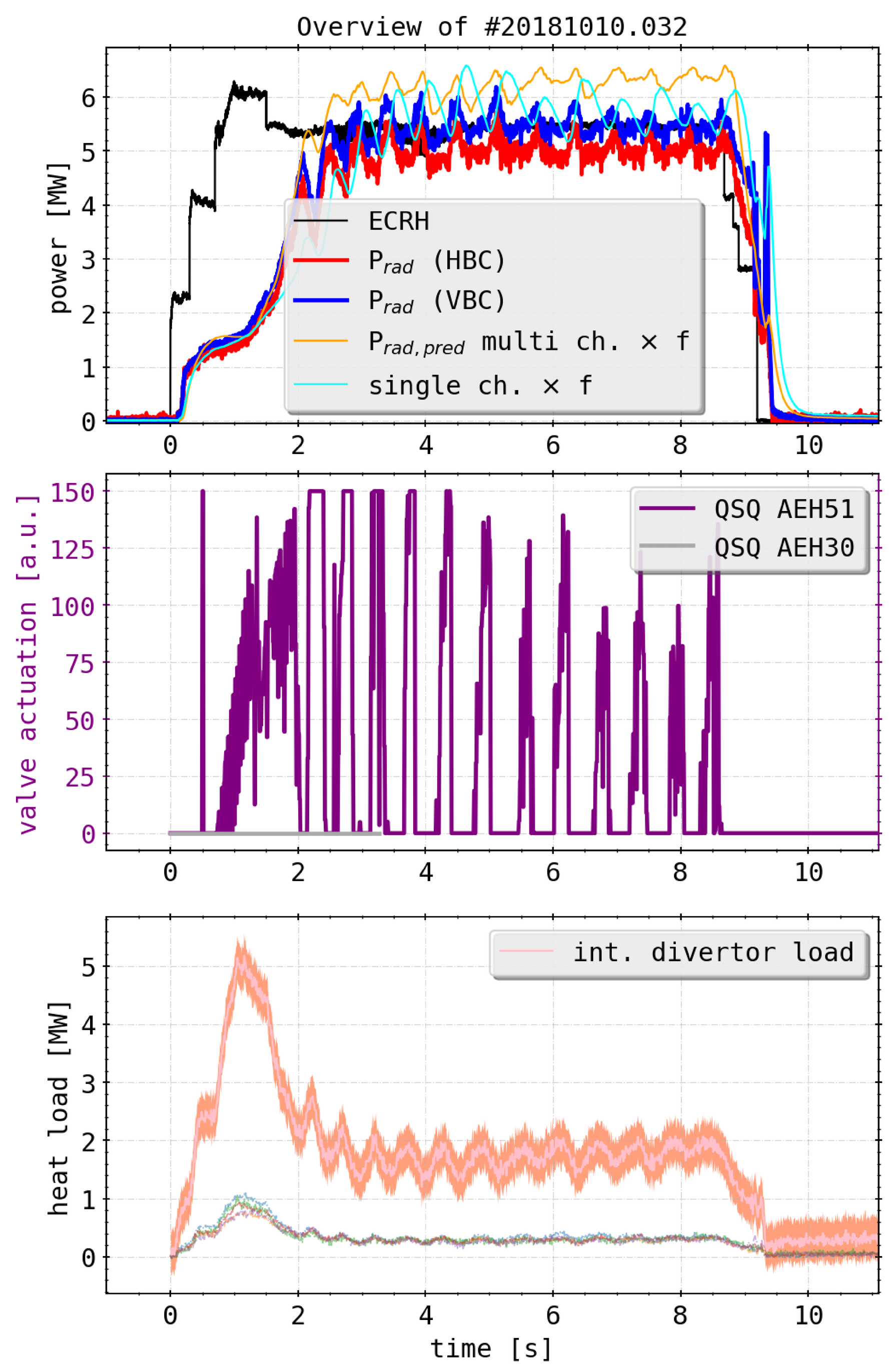

(top): Comparison of input heating power P_{ECR} and radiation power loss, as measured by the two camera arrays. Added are also the two feedback lines provided for the He beam valves. One features a predictive calculation like eq. (1), whereas the other uses one raw single channel signal multiplied by a manually adjusted factor. **(middle):** Valve actuation of the thermal He beam feedback actuator. This signal indicates whether and how far the valve has been opende to fuel hydrogen H_2 into the plasma. **(bottom):** Individual divertor module heat loads in W7-X (colored lines) and total integrated power.

Post-Feedback Sensitivity Evaluation

What combination of or individual channels S would have yielded the best feedback performance?

Using the prediction by a set S from eq. (1) one can define a *weighted (normalised) deviation*-like cost function as:

$$d_{\text{S}}(t) = \| P_{\text{rad, cam}}(t) - P_{\text{pred, S}}(t) \|$$

$$\varepsilon_{\text{S}}(t) = \begin{cases} 1 - \frac{d_{\text{S}}(t)}{P_{\text{rad, cam}}(t)} \ , & d_{\text{S}} < P_{\text{rad, cam}} \\ 0 & , \text{ else} \end{cases} \qquad (2)$$

$$\vartheta_{\text{S}} = \int_T \varepsilon_{\text{S}}(t) \mathrm{d}t \qquad (3)$$

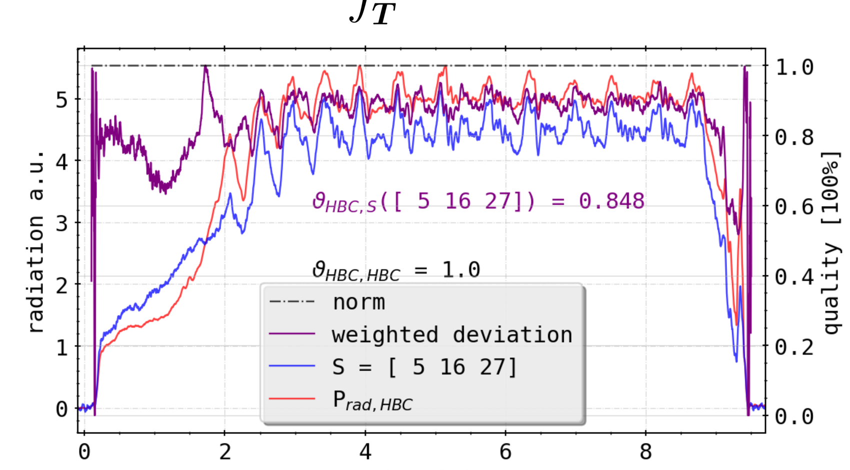

Comparison of P_{rad} from XPID: 20181010.032 as calculated from the LOS of the full HBC array and a trace example for the subset $S = \{5, 16, 27\}$ $P_{\text{pred, S}}$. The purple line is calculated using eq. (2), while the number $\vartheta_{\text{HBC, S}}$ is produced by eq. (3).

For example for $N_3 \sim 10^4$ subsets S_3 of $n = 3$ lines of sight $\vartheta_{\text{HBC, S}}$ has been calculated. Let N_{n}^{ch} be the number of S_{n}^{ch} where detector ch is incoorporated, the *average sensitivity of channel ch* becomes:

$$\Omega_{\text{ch}}^{\text{n}} = \frac{1}{N_{\text{ch}}^{\text{n}}} \sum_{s(ch)}^{N} \vartheta_{\text{HBC, s(ch)}} \qquad (4)$$

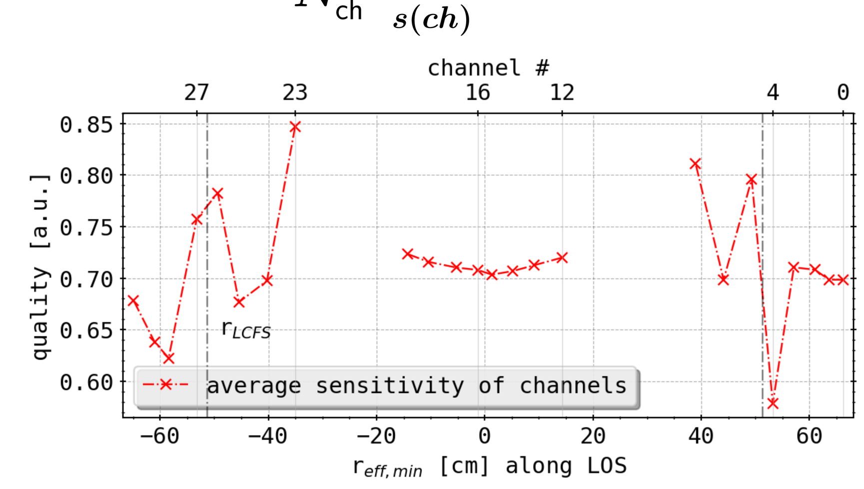

Results from eq. (4) for S_3 and XPID: 20181010.032. The abscissa is taken as the minimum effective plasma radius along the LOS of a detector. The combinatory space for the subsets has been restricted to reduce computational excess, which yields three distinguishable ranges on the left, center and right.

STRAHL Simulations of Carbon Radiation

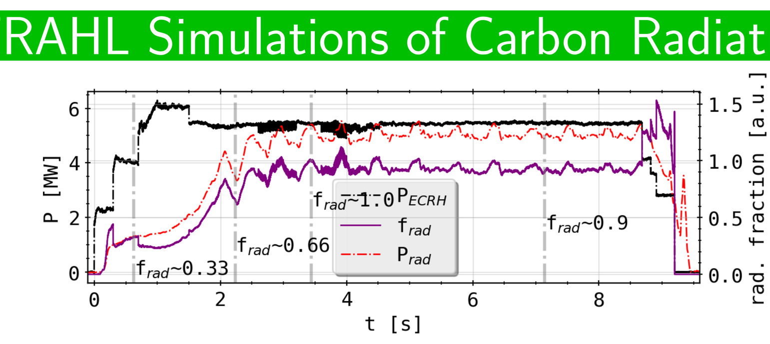

ECR heating power and $P_{\text{rad,HBC}}$ for radiation feedback controlled W7-X experiment XPID: 20181010.032. Indicated also the corresponding radiation power loss fraction $f_{\text{rad}} = P_{\text{ECR}}/P_{\text{rad}}$. For different radiation loss regimes f_{rad} has been marked.

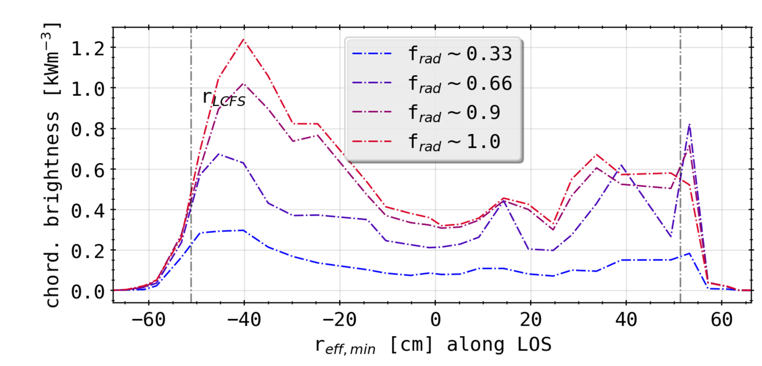

Chordal brightness profiles for the HBC camera array, noted over the minimum r_{eff} along the lines of sight, for points in time taken from the radiation fraction on the top.

- line-int. chordal profile shows majority of radiation coming from region close to separatrix or SOL
- increasing radiation fraction shows inward shift of brightness away from last closed fluxsurface

What causes this behaviour given the 1D radiation distribution and plasma profiles?

STRAHL:

- assuming 1D distribution, majority of radiation coming from inside LCFS
- impurity transport & radiation in coronal equilibrium modelled using *STRAHL* code and *ADAS* atomic database
- calculating radial transport $\Gamma_{\text{i,Z}}$ and emission of impurity i and ion-stage Z solving continuity equation using ansatz of anomalous diffusivities D^* and radial drift velocities v^*:

$$\frac{\partial n_{\text{i,Z}}}{\partial t} = -\nabla \Gamma_{\text{i,Z}} + Q_{\text{i,Z}}$$
$$= \frac{1}{r} \frac{\partial}{\partial r} r \left(D^* \frac{\partial n_{\text{i,Z}}}{\partial r} - v^* n_{\text{i,Z}} \right) + Q_{\text{i,Z}}$$

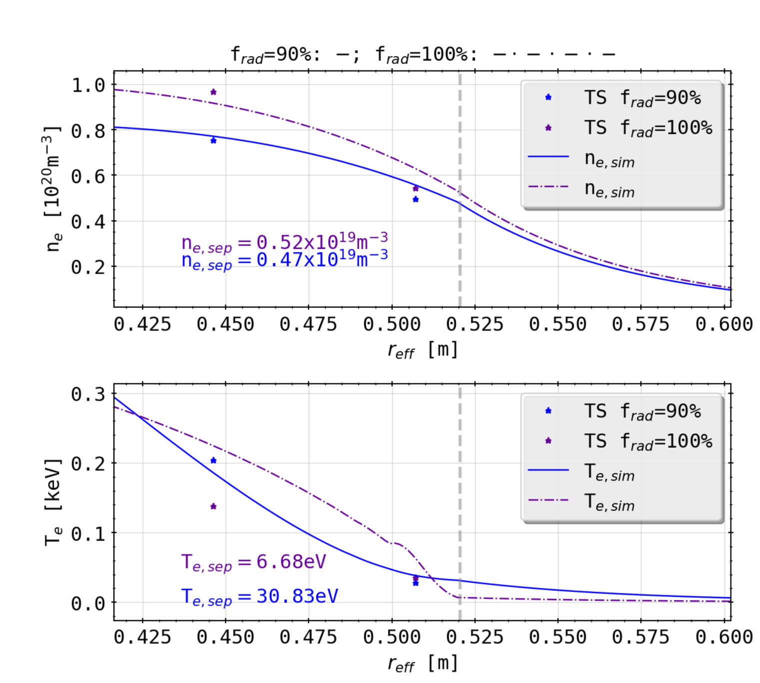

Thomson Scattering profiles for cases of high f_{rad}, as depicted in the top-page graph on XPID: 20181010.032, as well as spline-interpolated smooth traces for STRAHL input with exponentially decaying density & temperature beyond r_{LCFS}.

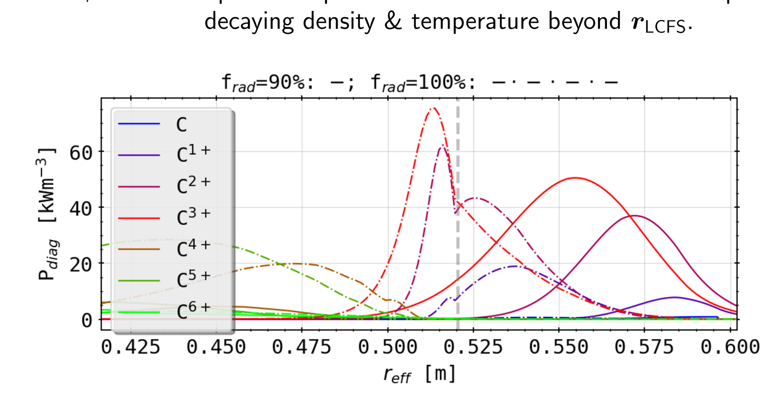

Line radiation for all ion stages C^{X+} of carbon in the coronal equilibrium according to the two radiation regimes shown above. When integrated for the plasma volume of W7-X the total radiation matches experimental levels.

Conclusions

- benchmarks using eq. (1) on different scenarios, cost metrics and camera/channels subsets (up to $n = 9$) show similar results
- Bolometer most sensitive to changes in radiation distribution along separatrix and SOL
- sensitivity analysis in STRAHL input parameters yields small changes in P_{diag}
- STRAHL shows strong radial dependence of intrinsic impurity radiation regarding temperature profile input
- carbon radiation possible indicator for regimes of detachment as main power sink

* Coresponding author: philipp.hacker@ipp.mpg.de

Deutsche Physikalische Gesellschaft - Spring Meeting Munich 2019, Matter and Cosmos Section (SMuK)

This work has been carried out within the framework of the EUROfusion Consortium and has received funding from the Euratom research and training programme 2014-2018 and 2019-2020 under grant agreement number 633053. The views and opinions expressed herein do not necessarily reflect those of the European Commission.